



Received on 22 June, 2017; received in revised form, 06 October, 2017; accepted, 20 October, 2017; published 01 April, 2018

PREPARATION AND PHYSIOCHEMICAL CHARACTERIZATION OF CHITOSAN NANOPARTICLES FOR CONTROLLED DELIVERY OF OXYTOCIN

Kimberly Anne Milligan, Cherese Winstead* and Jasmine Smith

Department of Chemistry, Delaware State University, 1200 N. DuPont Highway, Dover, Delaware 19901, USA.

Keywords:

Chitosan, Nanoparticles,
Oxytocin, Ionotropic gelation,
Triphosphate, Drug delivery

Correspondence to Author: Cherese Winstead

Department of Chemistry,
Delaware State University,
1200 N. DuPont Highway,
Dover, Delaware 19901, USA.


E-mail: cwinstead@desu.edu

ABSTRACT: This study aimed to characterize and evaluate chitosan nanoparticles (CSNPs) as a carrier system for the hormone, oxytocin. Ionotropic gelation was the technique used to synthesize the CSNPs. Scanning electron microscopy (SEM) and transmission electron microscopy (TEM) showed narrow particle size distribution of 30-50 nm and spherical particle shape. Differential scanning calorimetry (DSC), X-ray powder diffraction (XRD), thermal gravimetric / differential thermal analysis (TGA / DTA) and Fourier Transform Infrared Spectroscopy (FTIR) were used to evaluate possible drug-polymer interactions. Data obtained from X-ray diffraction (XRD) showed a decrease in crystallinity due to the disruption of the intramolecular / intermolecular chitosan network and a molecular level of oxytocin dispersion in the O-CSNP matrix. Differential scanning calorimetry (DSC) exhibited further evidence of drug-polymer interaction through observed endothermic shifts. Fourier-transform-infrared (FT-IR) spectra obtained confirmed the presence of oxytocin within the CSNP matrix as well as further proof of the intermolecular interactions existing between oxytocin and chitosan. Loading and release profiles of the O-CSNPs were conducted using LC/MS. The effect of nanoparticle size and oxytocin concentration was shown to affect drug loading capabilities and the release behaviour of the O-CSNPs under physiological conditions. *In vitro* release studies were also performed on the O-CSNPs, which exhibited an initial burst effect followed by first-order rate kinetics of oxytocin release from the system. In this work, CSNPs are presented as a potential carrier system for the extended release of oxytocin, thereby improving the efficacy of the hormone in the treatment of neurological disorders.

INTRODUCTION: Drug delivery systems using the biopolymer, chitosan, have attracted considerable attention due to the materials inherent biocompatibility, biodegradability, and non-toxic properties¹. Chitosan, one of the most copious biopolymers in nature, is derived from the exoskeleton of crustaceans such as crabs, shrimp, and lobsters as well as yeast and fungal walls of algae².

Derived from chitin, chitosan is composed of randomly distributed β -(1-4)-linked D-glucosamine (deacetylated unit) and N-acetyl-D-glucosamine (acetylated unit) repeating units³. Chitosan has a unique feature of adhering to the mucosal surface and transiently opening the tight junction between epithelial cells⁴. Thus, chitosan nanoparticles are potential delivery systems for hydrophilic drugs due to their outstanding physicochemical and biological properties⁵⁻⁷.

To date, a significant number of studies have focused on the controlled delivery of bioactive agents over conventional dosage methods, since they minimize side effects and prolong the efficacy of a drug, which in turn, reduces the frequency of drug administration⁸⁻¹⁰.

<p>QUICK RESPONSE CODE</p> 	<p>DOI: 10.13040/IJPSR.0975-8232.9(4).1430-1440</p>
<p>Article can be accessed online on: www.ijpsr.com</p>	
<p>DOI link: http://dx.doi.org/10.13040/IJPSR.0975-8232.9(4).1430-1440</p>	

Thus, nanoparticles have gained increasing attention given that the therapeutic index of almost any drug is enhanced through the use of nanotechnologies^{11, 12} as well as opportunities for non-invasive routes of administration such as oral, nasal and ocular¹³. Additionally, nanoparticles are advantageous as drug carriers due to their high stability; high transport capacity; expediency of both hydrophilic and hydrophobic substance integration; and feasibility of variable routes of administration, including oral administration and inhalation¹⁴. Nanoparticles can also be designed to enable controlled (sustained) drug release from the matrix¹⁵.

Many groups have studied chitosan nanoparticles (CSNPs) for its potential application in the delivery of anti-cancer drugs, antibiotics, peptides, genes, and proteins^{16, 17}. Over the years, CSNPs have been synthesized through various methods of ionotropic gelation, microemulsion, emulsification solvent diffusion, and polyelectrolyte complex^{18 - 20}. These methods offer straightforward and mild preparation techniques without the use of organic solvent or high shear force. CSNPs prepared by ionotropic gelation was first reported by Calvo *et al.*,²¹ and had been widely examined and developed^{22, 23}. In the method of ionotropic

gelation, positively charged amino groups on chitosan interact electrostatically with the negatively charged counterions resulting in spontaneous nanoparticle formation.

Oxytocin, a hormone synthesized in the hypothalamus, has been found to be beneficial in the treatment of autism and some neurological diseases such as depression and bipolar disorders²⁴. Oxytocin is critically involved in a wide variety of social behaviors in different species, including trust, controlling fear, facial recognition, and pair bonding²⁵. Studies have shown, however, that low levels of oxytocin are present in the blood plasma of subjects with neurological disorders. Although intranasal delivery of the hormone has improved many of the symptoms associated with these disorders^{26 - 27}, current therapeutic applications of oxytocin are limited by frequent doses and *in vivo* stability²⁸. Oxytocin is a neuropeptide made up of nine amino acids, which in solution exhibits the structure proposed by Urrey and Walter²⁹ in **Fig. 1**. To date, there exists little research in the area of controlled delivery of oxytocin using nanoparticles. As such, we present CSNPs as a potential carrier system for the extended the release of the hormone; thereby improving the efficacy of oxytocin treatments.

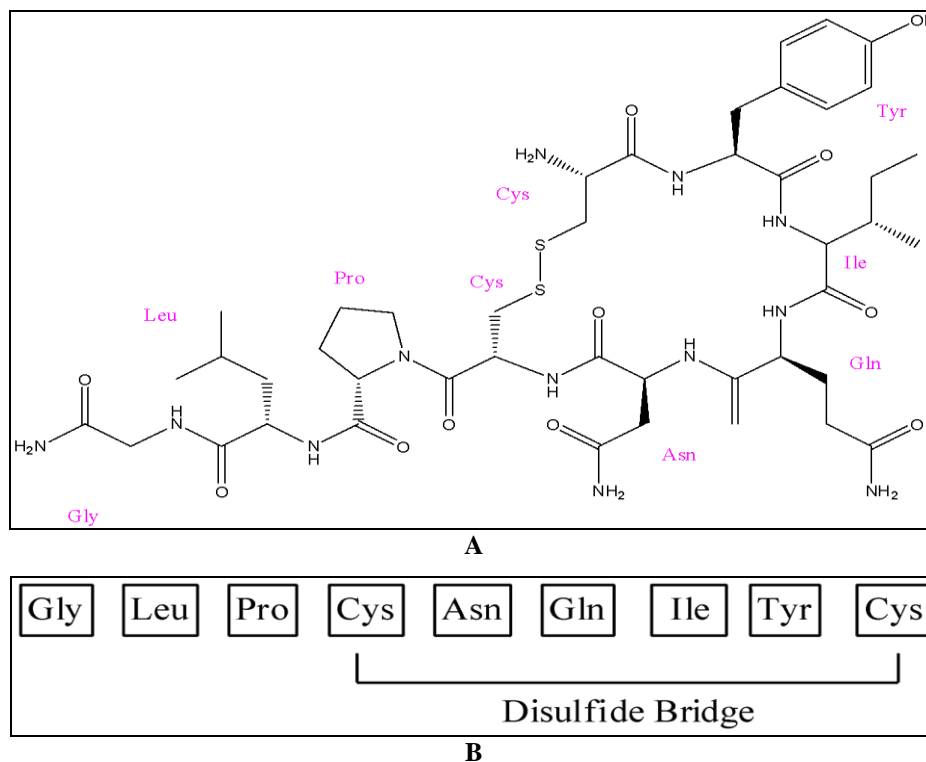


FIG. 1: CHEMICAL STRUCTURE OF OXYTOCIN (A) IN AQUEOUS SOLUTION (B) AMINO ACID SEQUENCE

MATERIALS AND METHODS:

Preparation of Oxytocin - loaded Chitosan Nanoparticles: Chitosan (medium molecular weight) and oxytocin were purchased from Sigma-Aldrich. Pentasodium tripolyphosphate (TPP) was obtained from Fisher. All other materials and reagents were of analytical grade and used without further purification.

Chitosan nanoparticles (CSNPs) were prepared *via* ionotropic gelation of chitosan with TPP, according to a traditional method described earlier by Rather *et al.*,³⁰. Briefly, chitosan (25 mg) was dissolved in 500 mL of 0.05% acetic acid to obtain a 0.005% (w/v) chitosan solution (pH 5.5 ± 0.1). Chitosan solution was added to 0.025% TPP aqueous solution (pH 5.4 ± 0.1) at a 1:1 ratio and stirred at room temperature for 15 minutes. A measured quantity (60 mg) of oxytocin was added and stirred for 2 hours in the chitosan solution before crosslinking for a final concentration of 0.12 mg/ml. The nanoparticles formed spontaneously and were then lyophilized for further characterization.

Particle Size and Morphology: Particle size and morphological examination of the oxytocin-loaded CSNPs was observed using a Hitachi 4700 scanning electron microscope (SEM) and a Zeiss Libra 120 transmission electron microscope (TEM) equipped with a Gatan Ultra scan 1000 2k x 2k CCD camera. Samples prepared for SEM examination were mounted onto aluminium stubs using double-sided adhesive tape and then sputter coated with a thin layer of gold in a vacuum. Aqueous dispersions of the particles were drop-cast onto a carbon-coated copper grid for TEM analysis, and the grid was air-dried at room temperature before loading.

Physicochemical Characterization: Infrared spectra were obtained using a Fourier transform infrared spectrophotometer (FT-IR, Nicolet 6700; Thermo Scientific), equipped with a reflectance ATR stage. Samples were scanned at a resolution of 4 cm⁻¹ from 400 - 4000 cm⁻¹. X-ray diffraction studies were conducted to investigate the crystalline nature of the system after encapsulation. Molecular arrangement of oxytocin and chitosan were compared by powder X-ray diffraction patterns acquired at room temperature on a Panalytical

X'Pert Siemens D5005 X-ray diffractometer using Cu K α radiation in the angle 2 θ range of 5 - 40 degrees. Thermostability studies were performed on a Perkin-Elmer Pyris Diamond Thermo-gravimetric / Differential Thermal Analyzer. For thermogram acquisition, sample sizes of 5 - 10 mg were scanned with a heating rate of 5 °C/min over a temperature range of 100 °C to 425 °C.

Loading Efficiency: The amount of oxytocin loaded in the CSNP matrix was characterized measuring the amount of oxytocin contained in the centrifugation supernatant and then calculating the loading efficiency using the following formula.

$$LE (\%) = \frac{\text{Total Oxytocin Used (IU/mL)} - \text{Free Oxytocin in Supernatant (IU/ml)} \times 100}{\text{Total Oxytocin Used (IU/mL)}}$$

Oxytocin in the supernatant was quantified using a Bruker ESQUIRE 3000 LC-MS system. One international unit (IU) of oxytocin is equivalent to 2 micrograms of the peptide. The oxytocin concentration range selected was based on the therapeutic values of treatment (18 - 24 IUs/dose).

The determination of the amount of oxytocin loaded in the chitosan nanoparticle was accomplished using LC/MS **Table 1**. An external method of calibration was used to determine the linearity of the analyte's response proportional to the concentration within specific ranges. The standard curve was linear between the ranges of 5 and 80 IUs (9.98 - 159.6 mg/ml).

TABLE 1: LC-MS PARAMETERS FOR LOADING AND RELEASE STUDIES

Parameters	Values
MS Parameters	
Source	Electrospray Ionization (ESI)
Capillary (kV)	4.5
End Plate Offset (kV)	0.5
Nebulizer (psi)	7.3
Dry Gas (l/min)	4.0
Dry Temperature (°C)	180
Polarity	Positive
ICC	Ultrascan
Target	200,000
Max. Accu. Time (ms)	200
Scan (m/z)	100-2800
Averages	5
LC Parameters	
Pump (mL/min)	0.2
Pressure (psi)	1800
Injection volume (μ l)	5

RESULTS: A proposed schematic for the binding of oxytocin to chitosan in the preparation of O-CSNPs is illustrated in **Fig. 2**, where oxytocin was incorporated into chitosan solution before crosslinking with tripolyphosphate (TPP) under acidic conditions. In solution, the following intramolecular hydrogen bonds are formed: C=O from Cys → N-H from Gly, Peptide C=O from Asn → N-H Tyr, and side chain C=O from Asn → N-H

Leu²⁹, which are unavailable for hydrogen bonding. In this work, it is proposed that the two available amino acids of Gln and Cys from oxytocin are available for intermolecular hydrogen bonding through the hydroxyl groups on the chitosan backbone. This interaction was studied using FTIR, XRD, and TGA/DTA. Morphology and particle size distribution were examined by SEM and TEM.

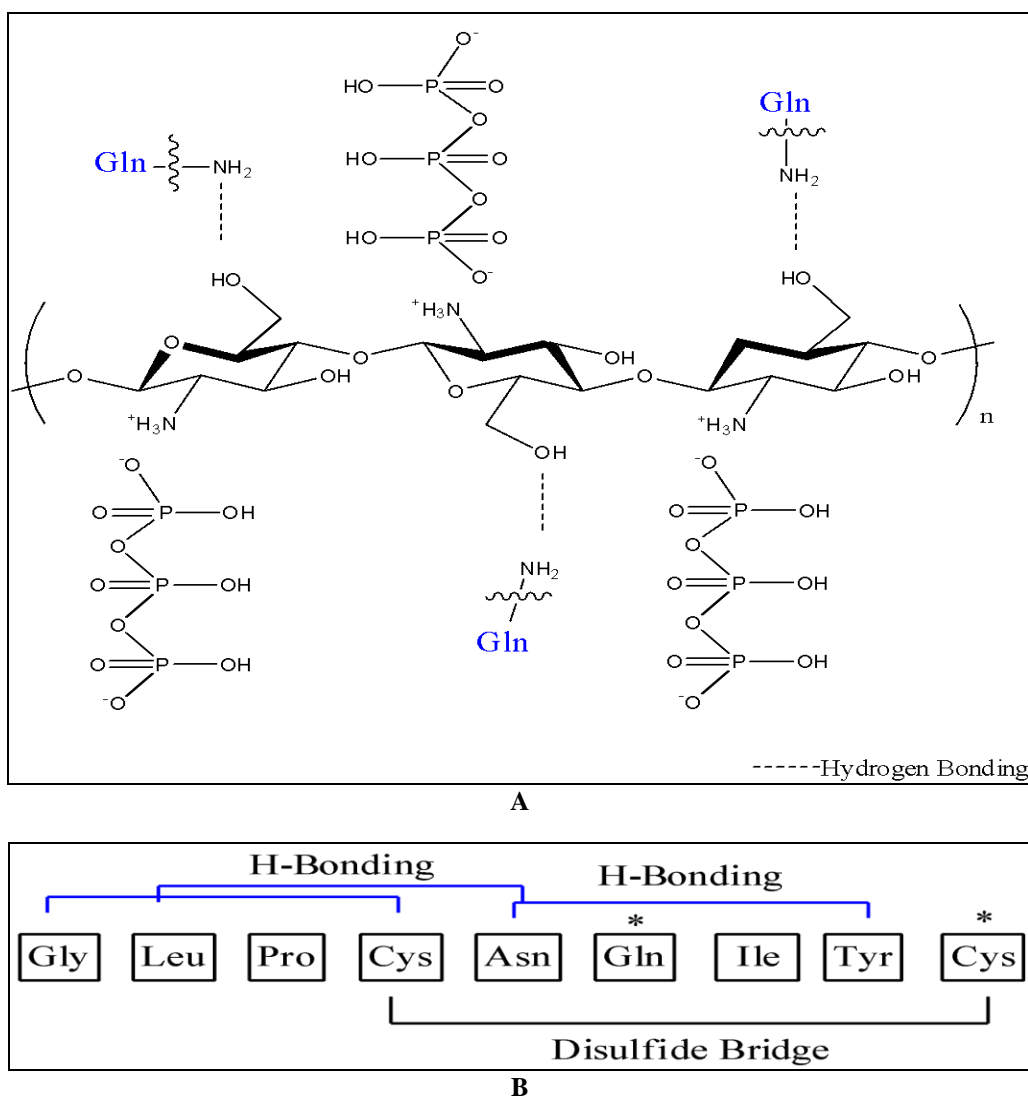


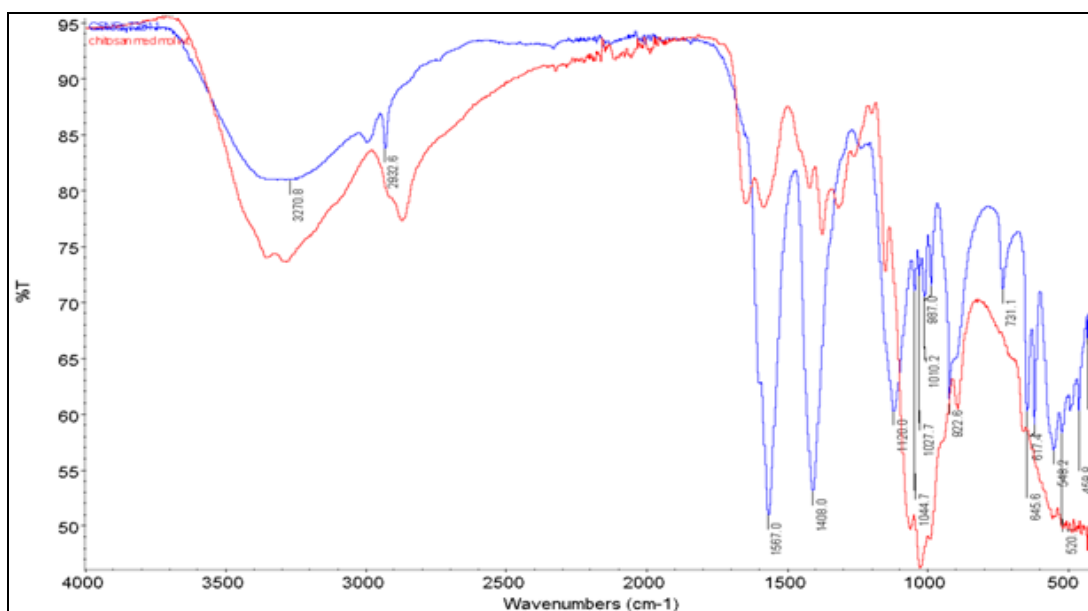
FIG. 2: PROPOSED SCHEMATIC OF OXYTOCIN-CHITOSAN INTERMOLECULAR INTERACTION (A) HYDROGEN BONDING EXISTING BETWEEN HYDROXYL GROUPS ON CHITOSAN AND GLY ON OXYTOCIN (B) AMINO ACID SEQUENCE DENOTING GLY AND CYS AMINO ACIDS AVAILABLE FOR HYDROGEN BONDING

Physicochemical Characterization: FTIR spectra in **Fig. 3A - C** show characteristic peaks of chitosan at 3429 cm⁻¹ for the -OH and -NH₂ group stretching vibrations as reported by Hosseinzadeh *et al.*,³¹. A peak at 1645 cm⁻¹ is due to the carbonyl stretching vibration in amide group (amide I vibration), and the peak at 1583 cm⁻¹ is due to N-H

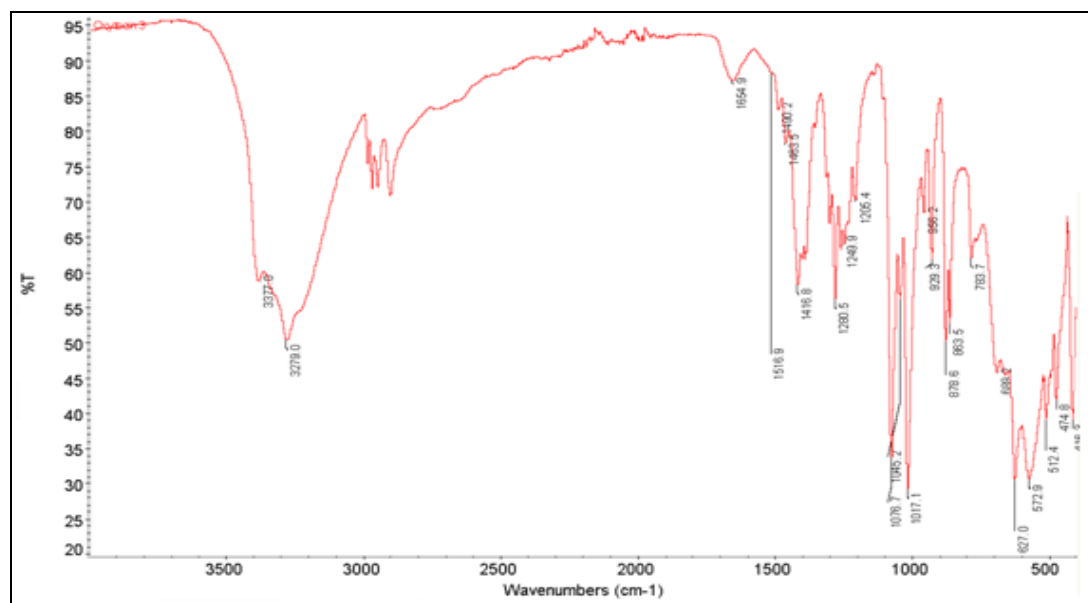
bending vibrations of the secondary amide. Absorption bands in the region of 1149 cm⁻¹ and 1031 cm⁻¹ are representative of anti-symmetric stretching of the C-O-C bridge and C-O stretching vibrations, which are characteristic of the chitosan saccharide structure as previously reported³¹. Upon formation of chitosan nanoparticles (CSNPs)

crosslinked with TPP, a small band at 1215 cm^{-1} is observed due to the stretching vibrations of $\text{P}=\text{O}$ as previously reported by Gierszewska-Drużyńska³². The peak shift from 1583 cm^{-1} to 1567 cm^{-1} represents the $-\text{NH}_2$ bending vibration, which was attributed to the linkage between tripolyphosphoric and ammonium group of NH_3^+ of chitosan. The FTIR spectra of oxytocin exhibits characteristic peaks of amide II stretching, which ranges from 1520 to 1580 cm^{-1} as a result of N-H and N-C deformations of the backbone peptide groups. The amide I region is observed at 1620 to 1700 cm^{-1} caused by the carbonyl stretching of the backbone peptide groups. A smaller absorbance at 1510 cm^{-1}

caused by the tyrosine side chain O-H deformation is also observed. The presence of the oxytocin disulfide bridge (C-S-S-C) is evident by the bands occurring from $570 - 705\text{ cm}^{-1}$ ¹³³. FTIR spectra of oxytocin loaded chitosan nanoparticles (O-CSNPs) confirm drug-polymer interaction through the observation of increased hydrogen bonding between the hydroxyl groups on chitosan and available amino acid groups of oxytocin as evidenced by the broadened OH stretching at 3400 cm^{-1} and a shift in the -OH deformation stretch from 887 cm^{-1} to 922 cm^{-1} . The presence of oxytocin in O-CSNPs was observed in the native disulfide stretch within the $570 - 705\text{ cm}^{-1}$ range.



A



B

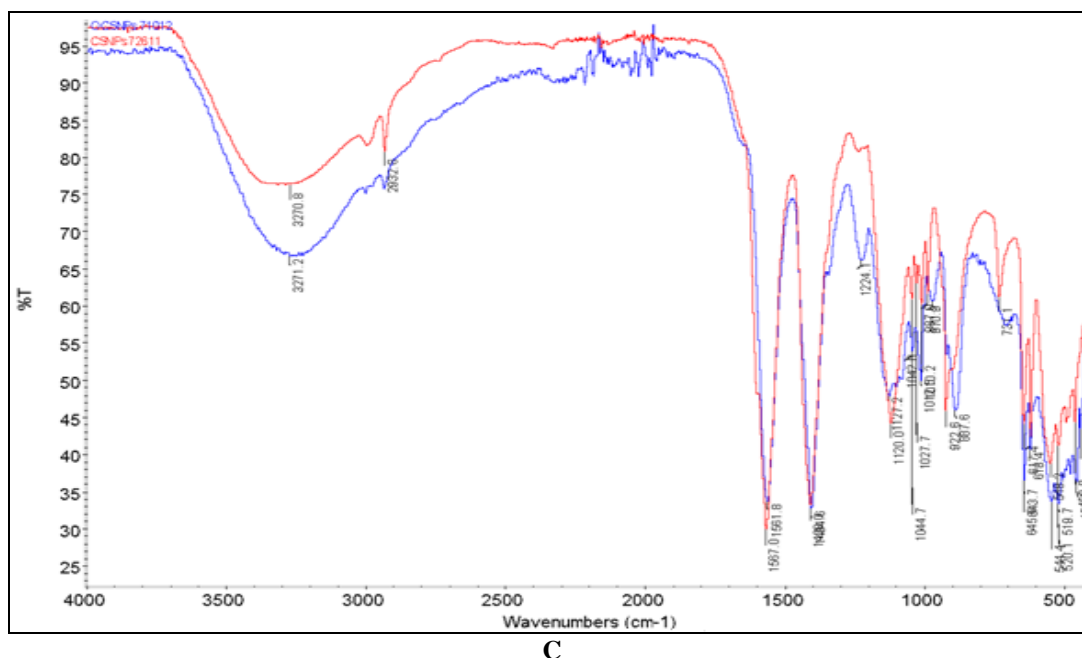


FIG. 3: FTIR SPECTRA OVERLAY (A) CHITOSAN (RED) AND CSNPs (BLUE) (B) SPECTRA OF OXYTOCIN (C) OVERLAY OF CSNPs (RED) AND O-CSNPs (BLUE)

X-ray diffraction (XRD) was used to analyze the degree of crystallinity and physical state of oxytocin once incorporated into the polymeric nanoparticles. XRD patterns of oxytocin, CSNPs, and O-CSNPs were obtained and compared and revealed significant differences in the molecular state of oxytocin once incorporated into the CSNP matrix. Native chitosan powder exhibits a broad characteristic peak at 20° (2θ), which is indicative of the predominantly amorphous form of chitosan³². As observed in the inset view of **Fig. 4**, the intensity of this peak is decreased and shifted slightly upon crosslinking with TPP, indicating a less crystalline structure imparted to the CSNPs. As reported previously, this decrease in crystalline structure is due to the intermolecular and

intramolecular network structure of CS, which when crosslinked by TPP counter ions, causes a disarray in chain alignment and subsequent decrease in crystallinity³⁴. In the case of oxytocin, the diffractogram exhibited several sharp crystalline peaks at the following 2θ values: 22°, 28°, 31°, 33°, 35°, and 38°. Upon loading of oxytocin, CSNPs became more amorphous. It is surmised that the observed decrease in crystallinity was due to the changes in the supramolecular structure of chitosan nanoparticles, which result from the formation of intermolecular hydrogen bonding between chitosan and oxytocin as well as from the breaking of chitosan intramolecular hydrogen bonds.

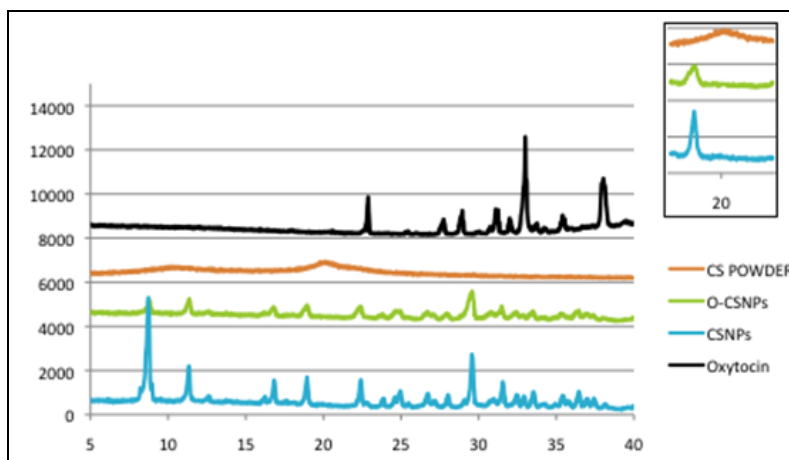


FIG. 4: XRD OF CS POWDER (ORANGE), CSNPs (BLUE), O-CSNPs (GREEN), AND OXYTOCIN (BLACK)

Effect of cross-linking and oxytocin loading on thermal stability of chitosan was studied by thermogravimetry and differential thermal analysis (TGA/DTA). As shown in **Fig. 5**, native CS exhibits an initial loss of water below 100 °C and an onset of degradation at 275 °C. The thermostability of the system was shown to decrease upon crosslinking. Denuziere *et al.*,³⁵ also reported the same findings and attributed the lowering of chitosan thermal stability to the changes in the molecular structure after crosslinking. DTA of CSNPs, oxytocin, and O-CSNPs were carried out to confirm drug-polymer interactions. The DTA for pure oxytocin revealed an endothermic melting peak at 166.61 °C. The DTA of CSNPs shows the appearance of two

shouldering endotherms at 105.02 and 121.39 °C and the degradation temperature of 313.89 °C that can be ascribed, respectively, to hydrogen-bonding dissociation and degradation. When compared to that of O-CSNPs, the two endotherms at 105.02 °C and 121.39 °C coalesce, and there is a small exothermic peak shift from 235.88 °C to 242.04 °C (as shown in the inset in **Fig. 5**). These shifts are evidence of oxytocin-chitosan interaction, which is most likely due to hydrogen bonding between the two available amino acid groups of oxytocin (Gln and Cys1) and hydroxyl groups on chitosan as proposed in **Fig. 2**. The disappearance of the oxytocin endothermic peak in O-CSNPs confirms low levels of free hormone exist in the loaded nanoparticles.

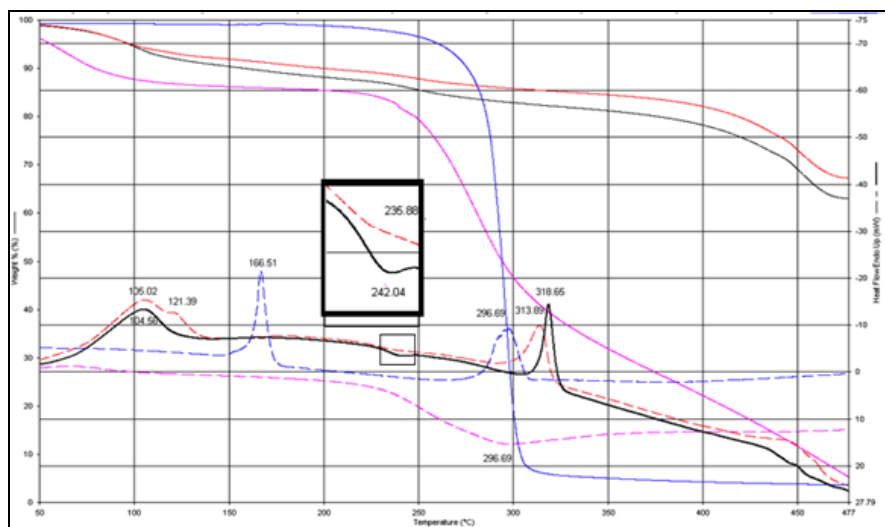
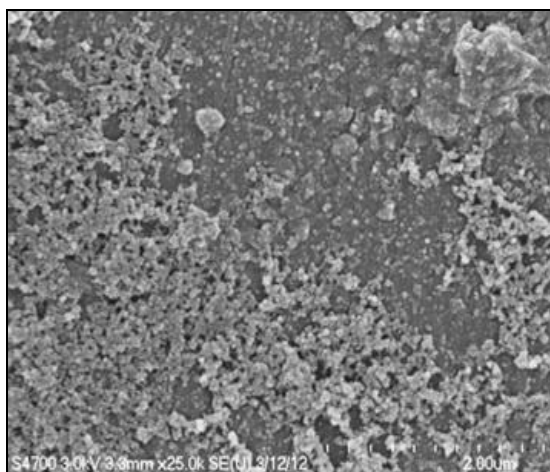


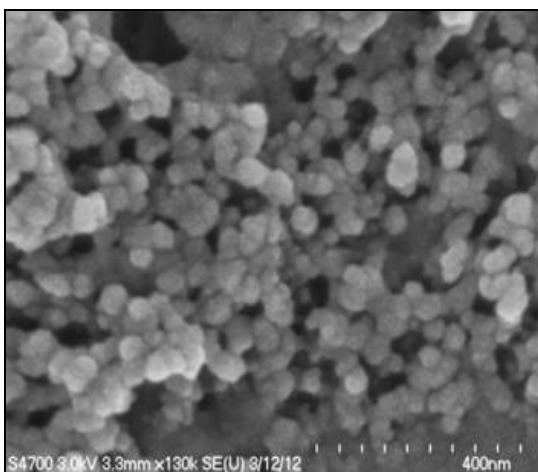
FIG. 5: TGA / DTA OF CHITOSAN, OXYTOCIN (BLUE), CS POWDER (PINK), CSNPs (RED), AND O-CSNPs (BLACK)

Scanning electron micrographs of CSNPs are shown in **Fig. 6A - D**. CSNPs were observed to be spherical with an average size of about 30 - 50 nm.

TEM confirmed that CSNPs were spherical with a uniform size distribution **Fig. 7A, B**.



A



B

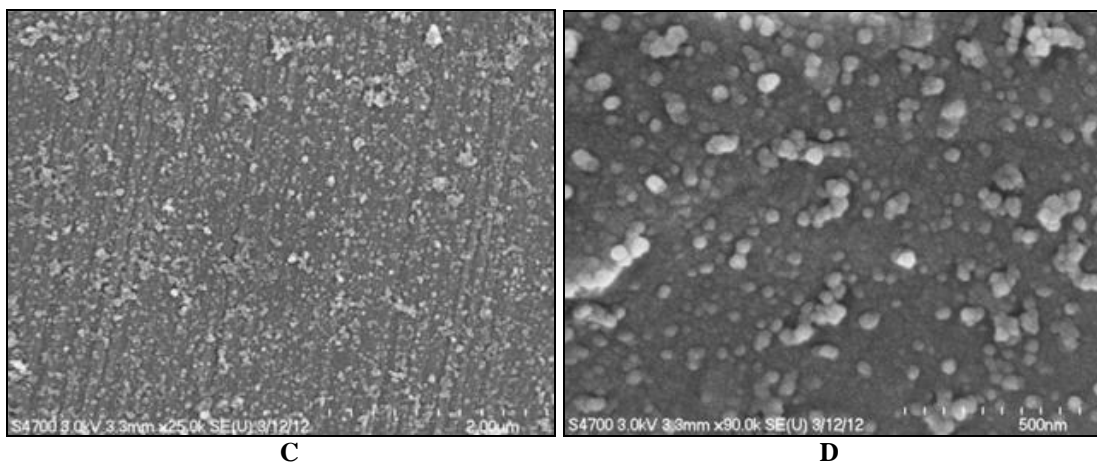


FIG. 6: SCANNING ELECTRON MICROGRAPHS OF CSNPs A) 40K, B) 150K, C) 40K, D) 150K MAGNIFICATIONS

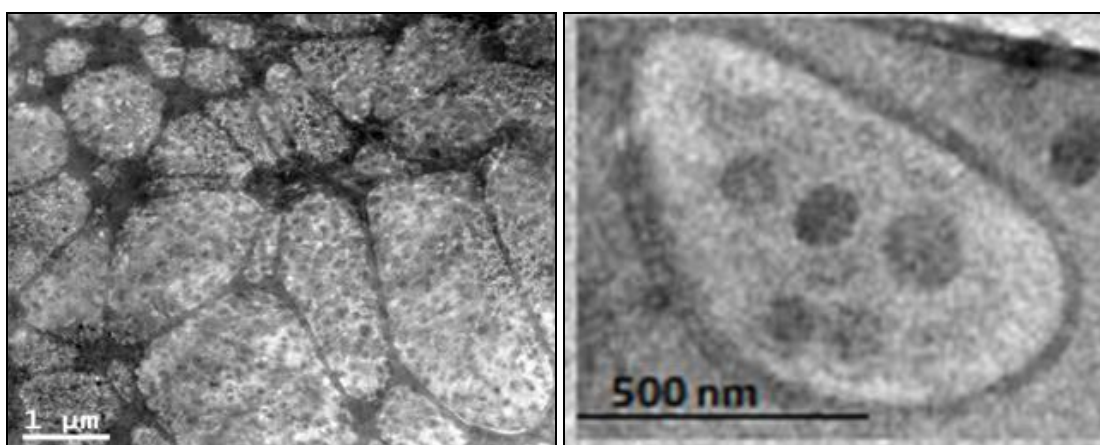


FIG. 7: TRANSMISSION ELECTRON MICROGRAPHS OF CSNPs 40 K MAGNIFICATION (LEFT) AND 150 K MAGNIFICATION (RIGHT)

Loading: CSNPs were loaded with oxytocin at various concentrations (10 - 30 IU/ml) to find the optimal loading efficiency. This range was selected based on the therapeutic range of oxytocin used in biomedical applications. The loading efficiency of the CSNPs is inversely related to oxytocin concentration up to about 25 IU/ml Fig. 8, which was determined to be the optimal loading concentration.

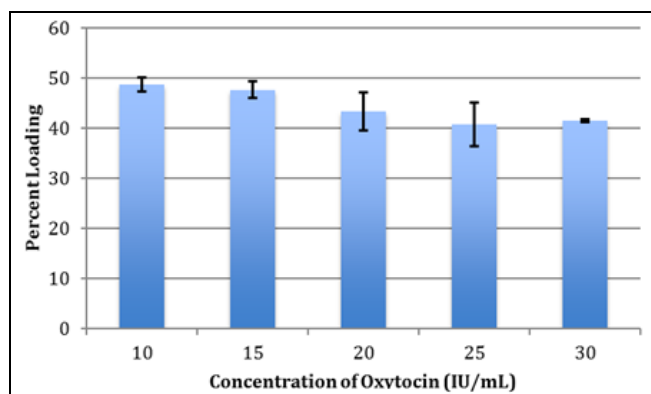


FIG. 8: LOADING EFFICIENCY OF CSNPs

The effect of particle size on loading efficiency was also observed Fig. 9, and it was determined that larger particles have fewer available sites for oxytocin binding, whereas smaller particles have more sites available for oxytocin-chitosan interaction due to a higher surface area. When the nanoparticle size was optimized to 50 nm, the loading capacity was shown to increase to 90% Fig. 9.

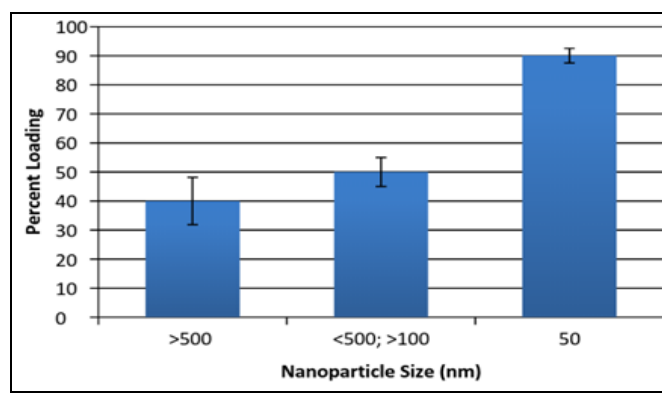


FIG. 9: THE EFFECT OF PARTICLE SIZE ON LOADING EFFICIENCY (OXYTOCIN CONCENTRATION 25 IU/mL)

Release Studies: Oxytocin-loaded CSNPs (O-CSNPs) were centrifuged, and the supernatant was separated by LC and identified by EI-MS at various times over 24 - 72 hr. **Table 2** shows the EI mass spectra data of oxytocin released into the supernatant from single - crosslinked CSNPs at different intervals. The UV quantifies the concentration at which oxytocin was released into

the supernatant in tandem with MS, which confirmed the target analyte. No release of oxytocin is observed (A, B) until after 1 hour when a 'burst' (32.3%) effect of oxytocin occurs as shown in Table 2. This amount (32.3 - 38.5%) is sustained (C, D, E) for up to 24 hours, after which elevated levels of oxytocin is observed due to the erosion of the CSNP matrix.

TABLE 2: RELEASE PROFILE OF O-CSNPs

	Time (hours)	Target Analyte	Extracted Ion Peak Mass (m/z)	Retention Time (min)	Mean Absorbance (mAU)	% Release	Standard Deviation
A	0	Oxytocin	1007.5	0	0	0	0
B	0.5	Oxytocin	1007.5	0	0	0	0
C	1	Oxytocin	1007.5	7.4	19.3	32.3	3.1
D	1.5	Oxytocin	1007.5	7.4	3.3	37.8	2.6
E	24	Oxytocin	1007.5	7.4	0.4	38.5	1.5
NS	48	Oxytocin	1007.5	7.4	2.9	43.3	5.8
NS	72	Oxytocin	1007.5	7.4	25.2	85.3	5.5

*NS- Not shown due to degradation of CSNP matrix. LC-UV and MS are run in tandem

In vitro Release Profile of Oxytocin from CSNPs using LC-MS: *In vitro* dissolution testing using phosphate buffered saline is an essential well-characterized method for screening drug formulations before moving onto *in vivo* studies that evaluate the efficacy of the delivery system. The release profile of oxytocin-loaded CSNPs (O-CSNPs) was investigated under physiological conditions using phosphate buffered saline (pH 7) over 72 hours to evaluate the rate at which oxytocin was released from the chitosan nanoparticles and to quantify the number of days the hormone remained stable before degradation occurred. The hormone release from TPP-crosslinked CSNPs (O-CSNPs) showed 40% of the hormone was released over a 24 hour period.

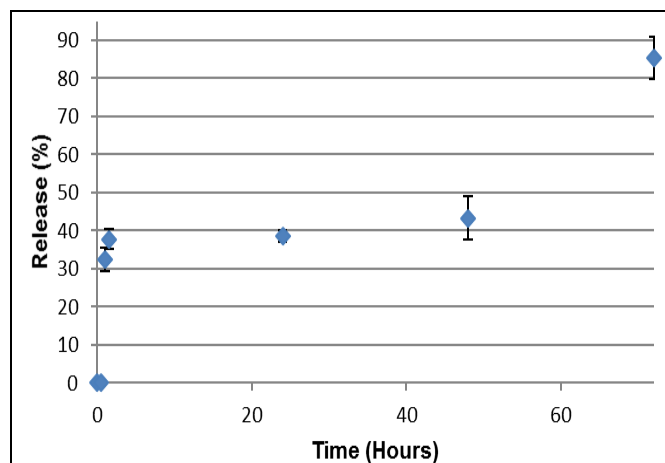


FIG. 10: THE RELEASE PROFILE OF OXYTOCIN FROM CSNPs SINGLE - CROSSLINKED WITH TPP OVER 72 HOURS

The initial rapid drug release from the single-crosslinked nanoparticles was due to the release of oxytocin from the surface of the nanoparticle. A similar release profile was reported by Elgadir *et al.*,¹³ for the release of silver sulfadiazine from a bilayer chitosan dressing that exhibited a burst release on the day one and then abated to a much slower release. Nallamuthu *et al.*, also reported the sustainable release of chlorogenic acid from crosslinked chitosan nanoparticle³⁶.

CONCLUSION: This study demonstrates a rapid, mild method for preparing oxytocin - loaded chitosan nanoparticles. Morphology and particle size using SEM and TEM show nanospherical particles ranging from 30 - 50 nm in size. XRD patterns showed a molecular dispersion of oxytocin within the CSNP matrix and an observed decrease in crystallinity upon crosslinking and loading of oxytocin due to the disruption in the intramolecular / intermolecular chitosan network. FTIR and TGA / DTA confirmed oxytocin - chitosan intermolecular interaction. Results support the hypothesis that chitosan nanoparticles could be a valuable tool in the controlled-release of hormones for therapeutic applications.

The loading efficiency of oxytocin onto the CSNPs was studied as an effect of particle size and results showed that the loading capacity of the nanoparticles is inversely related to the size. A maximum loading capacity of 90% was attained

upon particle size reduction to 50 nm. Release studies were performed and involved the following 3-stage release profile: burst, sustained, erosion. The O-CSNPs showed an initial burst effect within the initial 24hr period due to the release of surface adsorbed oxytocin, followed by a sustained period of release of oxytocin from the pores and channels of the nanoparticles, and final erosion of the chitosan matrix at 72 hours.

With the development of a CSNP matrix exploiting the intermolecular hydrogen bonding between the amine groups of chitosan and available amino acids of oxytocin, the effects of oxytocin are sustained longer under physiological conditions. By optimizing of the intermolecular bonding of chitosan nanoparticles, we have enhanced oxytocin stability under physiological conditions for a prolonged period. This enhanced stability, in turn, will increase the length of time chitosan is adsorbed to the mucosal lining of the nasal cavity, which will increase the bioavailability and absorption of oxytocin.

ACKNOWLEDGEMENT: The authors gratefully acknowledge the Center for Hydrogen Storage, Delaware Biotechnology Institute (DBI), the Applied Optics Center for Instrumental Facilitation. Special thanks to Adeola Ibikunle and Samuel Orefuwa for your valuable advice and expertise. Financial supports from IDeA Networks of Biomedical Research Excellence (INBRE), NASA Delaware Space Grant and Experimental Program to Stimulate Competitive Research (EPSCoR) are highly appreciated.

CONFLICT OF INTEREST: The authors declared no competing interests.

REFERENCES:

1. Laskar K and Rauf A: Chitosan-based nanoparticles towards biomedical applications. *Nanomed Res J* 2017; 5(2): 00112.
2. Younes I and Rinaudo M: Chitosan and chitosan preparation from marine sources. Structures, properties, and applications. *Mar. Drugs* 2015; 13(3): 1133-1174. doi:10.3390/md13031133
3. Cheung RCF, Ng TB, Wong JH and Chan WY: Chitosan: An update on potential biomedical and pharmaceutical applications. Laurienzo P, ed. *Mar. Drugs* 2015; 13(8): 5156-5186. doi:10.3390/md13085156.
4. Zhang J, Zhu X, Jin Y, Shan W and Huang Y: Mechanism study of cellular uptake and tight junction opening mediated by goblet cell-specific trimethyl chitosan

- nanoparticles. *Mol. Pharm* 2014; 11(5): 1520-1532. doi: 10.1021/mp400685v.
5. Jung WJ and Park RD: Bioproduction of chitoooligo saccharides: Present and perspectives. *Mar. Drugs* 2014; 12: 5328-5356.
6. Walke S, Srivastava G, Nikalje M, Doshi J, Kumar R, Ravetkar S and Doshi P: Physicochemical and functional characterization of chitosan prepared from shrimp shells and investigation of its antibacterial, antioxidant and tetanus toxoid entrapment efficiency. *International Journal of Pharmaceutical Science Review and Research* 2014; 26(2): 215-222.
7. Zhang J, Li C, Xue ZY, Cheng HW, Huang FW, Zhuo RX and Zhang XZ: Fabrication of lactobionic-loaded chitosan microcapsules as potential drug carriers targeting the liver. *Acta Biomaterialia* 2011; 7(4): 1665-1673.
8. Najafi S, Pazhouhnia Z, Ahmadi O, Berenjian A and Jafarizadeh-Malmiri H: Chitosan nanoparticles and their applications in drug delivery: A review. *Current Research in Drug Discovery* 2014; 1(1): 17-25.
9. Elgadir A, Uddin S, Ferdosh S, Adam A, Khan AJ and Sarker ZI: Impact of chitosan composites and chitosan nanoparticle composites on various drug delivery systems. *J Food Drug Anal* 2015; 23(4): 619-629.
10. Rodrigues S, Dionísio M, López CR and Grenha A: Biocompatibility of chitosan carriers with application in drug delivery. *J Funct Biomater* 2012; 3: 615-641.
11. Poonia N, Kharb R, Lather V and Pandita D: Nanostructured lipid carriers: Versatile oral delivery vehicle. *Future Sci OA* 2016; 2(3): FSO135. doi: 10.4155/fsoa-2016-0030.
12. Vicario-de-la-Torre M and Forcada J: Review the potential of stimuli-responsive nanogels in drug and active molecule delivery for targeted therapy. *Gels* 2017; 3(16): 1-37.
13. Patel A, Patel M, Yang X and Mitra AK. Recent Advances in Protein and Peptide Drug Delivery: A Special Emphasis on Polymeric Nanoparticles. *Protein and Peptide Letters* 2014; 21(11): 1102-1120.
14. Bhatia S: *Nanotechnology in Drug Delivery*. Apple Academic Press 2016.
15. Sun L, Chen Y, Zhou Y, Guo D, Fan Y, Guo F, Zheng Y and Chen W: Preparation of 5-fluorouracil-loaded chitosan nanoparticles and study of the sustained release *in vitro* and *in vivo*. *Asian Journal of Pharmaceutical Sciences* 2017; 12(5): 418-423.
16. Ding RL, Xie F, Hu Y, Fu SZ, Wu JB, Fan J, He WF, He Y, Yang, LL, Lin S and Wen QL: Preparation of endostatin-loaded chitosan nanoparticles and evaluation of the antitumor effect of such nanoparticles on the Lewis lung cancer model. *Drug Delivery* 2017; 24(1): 300-308. doi: 10.1080/10717544.2016.1247927.
17. Xiao YF, Jie MM, Li BS, Hu CJ, Xie R, Tang B and Yang SM: Peptide-Based Treatment: A Promising Cancer Therapy. *Journal of Immunology Research* 2015; 1-13. Article ID 761820. doi:10.1155/2015/761820.
18. Rajitha P, Gopinath D, Biswas R, Sabitha M and Jayakumar R: Chitosan nanoparticles in drug therapy of infectious and inflammatory diseases. *Expert Opinion on Drug Delivery* 2016; 13(8): 1177-1194. Doi:10.1080/17425247.2016.1178232.
19. Rajalakshmi R, Muzib Y, Aruna U, Vinesha V, Rupangada V and Krishna Moorthy SB: Chitosan nanoparticles – An emerging trend in nanotechnology. *International Journal of Drug Delivery* 2014; 6: 204-229.
20. Sharma G, Sharma AR, Nam JS, Doss GPC, Lee SS and Chakrabo C: Nanoparticle-based insulin delivery system:

- The next generation efficient therapy for Type 1 diabetes. *Journal of Nanobiotechnology* 2015; 13: 74.
21. Calvo P, Remuñan-López C, Vila-Jato JL and Alonso MJ: Chitosan and chitosan/ethylene oxide-propylene oxide block copolymer nanoparticles as novel carriers for proteins and vaccines. *Pharmaceutical Research* 1997; 14: 1431-1436.
 22. Desai KG: Chitosan nanoparticles prepared by ionotropic gelation: An overview of recent advances. *Critical Reviews in Therapeutic Drug Carrier Systems* 2016; 33(2): 107-58.
 23. Kouchak M and Azarpanah A: Preparation and *in vitro* evaluation of chitosan nanoparticles containing diclofenac using the ion-gelation method. *Jundishapur Journal of Natural Pharmaceutical Products* 2015; 10(2): e23082.
 24. Anagnostou E, Soorya L, Brian J, Dupuis A, Mankad D, Smile S and Jacob S: Intranasal oxytocin in the treatment of autism spectrum disorders: A review of literature and early safety and efficacy data in youth. *Brain Research* 2014; 1580: 188-198.
 25. Lieberwirth C and Wang Z: Social bonding: regulation by neuropeptides. *Frontiers in Neuroscience* 2014; 8: 171. doi:10.3389/fnins.2014.00171.
 26. Quattrocki E and Friston K: Autism, oxytocin and interoception. *Neuroscience and Biobehavioral Reviews* 2014; 47: 410-430. doi:10.1016/j.neubiorev.2014.09.012.
 27. Macdonald K and Macdonald TM: The Peptide that Binds: A systematic review of oxytocin and its pro-social effects in humans. *Harvard Review of Psychiatry* 2010; 18(1): 1-21.
 28. Cochran D, Fallon D, Hill M and Frazier JA: The role of oxytocin in psychiatric disorders: A review of biological and therapeutic research findings. *Harvard Review of Psychiatry* 2013; 21(5): 219-247. doi:10.1097/HRP.0b013e3182a75b7d.
 29. Urey DW and Walter R: Proposed conformation of oxytocin in solution. *Proceedings of the National Academy of Science* 1971; 68(5): 956-958.
 30. Rather MA, Sharma R, Gupta S, Ferosekhan S, Ramya VL and Jadhao SB: Chitosan-Nanoconjugated Hormone Nanoparticles for Sustained Surge of Gonadotropins and Enhanced Reproductive Output in Female Fish. Ceña V, ed. *PLoS ONE* 2013; 8(2): e57094. doi:10.1371/journal.pone.0057094.
 31. Hosseinzadeh H, Atyabi F, Dinarvand R and Ostad SN: Chitosan-pluronic nanoparticles as oral delivery of anticancer gemcitabine; Preparation and *in vitro* study. *International Journal of Nanomedicine* 2012; 7: 1851-1863.
 32. Gierszewska-Drużyńska M and Ostrowska-Czubenko J: The effect of ionic cross-linking on thermal properties of hydrogel chitosan membranes. *Progress in Chemistry and Applications of Chitin and Its Derivatives* 2010; (15): 25-32.
 33. Kalimuthu P, Kalimuthu P and John SA: Solvent-induced disulfide bond formation in 2, 5-dimercapto-1, 3, 4-thiadiazole. *Nature Proceedings* 2007.
 34. Yousefpour P, Atyabi F, Vashghani-Farahani E, Movahedi AA and Dinarvand R: Targeted delivery of doxorubicin-utilizing chitosan nanoparticles surface-functionalized with anti-HER2 trastuzumab. *International Journal of Nanomedicine* 2011; 6: 1977-1990.
 35. Denuziere A, Ferrier D, Damour O and Domard A: Chitosan-chondroitin sulfate and chitosan-hyaluronate polyelectrolyte complexes: Biological properties. *Biomaterials* 1998; 19(14): 1275-1285.
 36. Nallamuthu I, Devi A and Khanum F: Chlorogenic acid loaded chitosan nanoparticles with sustained release property, retained antioxidant activity and enhanced bioavailability. *Asian Journal of Pharmaceutical Sciences* 2015; 10(3): 203-211.

How to cite this article:

Milligan KA, Winstead C and Smith J: Preparation and physicochemical characterization of chitosan nanoparticles for controlled delivery of oxytocin. *Int J Pharm Sci Res* 2018; 9(4): 1430-1440. doi: 10.13040/IJPSR.0975-8232.9(4).1430-1440.

All © 2013 are reserved by International Journal of Pharmaceutical Sciences and Research. This Journal licensed under a Creative Commons Attribution-NonCommercial-ShareAlike 3.0 Unported License.

This article can be downloaded to **ANDROID OS** based mobile. Scan QR Code using Code/Bar Scanner from your mobile. (Scanners are available on Google Playstore)